Journal of Food Engineering 240 (2019) 191–198

Contents lists available at ScienceDirect

Journal of Food Engineering

journal homepage: www.elsevier.com/locate/jfoodeng

Chitosan thymol nanoparticles improve the antimicrobial effect and the water vapour barrier of chitosan-quinoa protein films

Estefanía Medina[a], Nelson Caro[a,b], Lilian Abugoch[a,**], Alexander Gamboa[a], Mario Díaz-Dosque[c], Cristian Tapia[a,*]

[a] Departamento de Ciencia de Los Alimentos y Tecnología Química, Facultad de Ciencias Químicas y Farmacéuticas, Universidad de Chile, Santos Dumont 964, Santiago, Chile, Santiago, Chile
[b] Centro de Investigación AustralBiotech-Universidad Santo Tomas, Avenida Ejército 146, 2° Subsuelo Edificio C, Santiago, Chile
[c] Facultad de Odontología, Universidad de Chile, Santiago, Chile

ARTICLE INFO

Keywords:
Chitosan
Quinoa protein
Nanoparticles
Edible films
Food packaging

ABSTRACT

The aim of this work was to improve the performance of quinoa protein/chitosan edible films on the extension of postharvest life of blueberries and tomato cherries by addition of chitosan thymol nanoparticles prepared by ionic gelation. These nanoparticles were effective at inhibiting the mycelial growth of *Botrytis cinerea*. Films with nanoparticles were significantly more effective in reducing water vapour permeability than were films with sunflower oil and film control without nanoparticles. Films with nanoparticles were applied as an internal coating to a polyethylene terephthalate (PET) clamshell container to store blueberries and tomato cherries, and the weight loss was evaluated. The weight loss for both foods stored in modified PET clamshells was significantly lower than that in the unmodified PET clamshell during storage at 7 °C and 85% RH for 10 days. Thus, chitosan thymol nanoparticles have a potential application as an antimicrobial for preservation of fresh fruits and as a water vapour barrier when these particles are added into chitosan-quinoa protein films.

1. Introduction

Food packaging based on chitosan (C) films and coatings has been extensively studied for food preservation. In particular, our group has studied chitosan-quinoa protein complexes because two ecotypes of quinoa are present in Chile: Salare quinoa, in the country's north, and Coastal quinoa from sea-level areas in the central and south central region. In the central region where the country's highest poverty rates, quinoa is grown on family farms, however, it is the main producer area quinoa (53% relative to the total of Chile) (Fuentes et al., 2017). The ecotypes crop in this zone has good quality of protein and the highest antioxidant activity compared with the other ecotypes crop in Chile, but they have small size, and a bitter taste, which made them less competitive, compared with Bolivian/Chilean north sweet ecotypes (Bazile et al., 2014). On the other hand, structural properties determined by XRD, FTIR and TGA showed a clear interaction between quinoa proteins and chitosan (Abugoch et al., 2011). The quinoa protein extract (PE) is not a film-forming macromolecule by itself (Valenzuela et al., 2013a). When PE is mixed with chitosan, hydrogen bonding and other type of intermolecular interactions results in a new material with film-forming capacity with much higher elongation at break than chitosan (Abugoch et al., 2011). This property only can be attributed to the presence of protein, because in only those experiments where were added lipids, it was possible to detect hydrophobic interactions (Valenzuela et al., 2013b).

It is known that chitosan, a copolymer consisting of β-(1–4)-2-acetamido-D-glucose and β-(1–4)-2-amino-D-glucose units, has good antibacterial and antifungal properties (Hosseinnejad and Jafari, 2016; Muxika et al., 2017). But, chitosan has weak mechanical properties and limited water vapour barriers (Abugoch et al., 2011; Kerch, 2015).

One solution is the addition of lipids of oil in a range of concentration from 2.9% to 50% which decreased the water vapour permeability (WVP) of chitosan films by up to 20% but caused a significant decrease in the tensile strength (TS) of up to 80%, the elongation at break (E%) of up to 70%, and the elastic modulus of up to 28% compared to the films control (Morillon et al., 2002; Valenzuela et al.,

Abbreviation: CNPs, Chitosan Nanoparticles; CTNPs, Chitosan Timol Nanoparticles; CQF, Chitosan Quinoa Films; CQOF, Chitosan Quinoa Oil Films; CQTF, Chitosan Quinoa Timol Films (with nanoparticles); C, Chitosan; NPs, Nanoparticles; TPP, sodium tripolyphosphate; T, Thymol

* Corresponding author.
** Corresponding author.
E-mail addresses: labugoch@uchile.cl (L. Abugoch), ctapia@uchile.cl (C. Tapia).

https://doi.org/10.1016/j.jfoodeng.2018.07.023
Received 4 December 2017; Received in revised form 26 June 2018; Accepted 23 July 2018
Available online 25 July 2018
0260-8774/

2013a; b; Vargas et al., 2009). The other approach is to include nanoparticles (NPs) into the films. It is known that NPs have a tortuosity effect on the films due to the hydrogen bonding between them and the film matrix (Duncan, 2011). Depending on the type of NPs, the WVP can decrease by up to 50% compared to films without NPs (Dehnad et al., 2014; Muller et al., 2009), and their advantage is that they affect the mechanical properties less compared to films treated with lipids (Abdollahi et al., 2013; de Moura et al., 2009; Dehnad et al., 2014; Muller et al., 2009). Recently, it was reported that the use of edible coatings containing chitosan NPs obtained by ionic gelation is effective at delaying the ripening process of grapes (Melo et al., 2018). Besides, the use of chitosan and nano-SiOx coating increases the shelf life of Chinese cherries during postharvest storage (Xin et al., 2017). On the other hand, it has been proven that the incorporation of essential oils significantly increased the antibacterial and antifungal efficacy of chitosan films and coatings in vitro (Kerch, 2015). Thymol is the major antimicrobial agent of the aromatic plant thyme (*Thymus vulgaris*); it is a phenolic and hydrophobic compound capable of binding bacterial proteins and giving rise to the disintegration and permeability of the cell membrane and thus has a strong antimicrobial effect. So that thymol may be incorporated as a natural antifungal agent in an active package to increase shelf life of foods (Mirdehghan and Valero, 2017). Recently, researchers evaluated the antifungal effect of thymol nanoemulsions incorporated into quinoa protein/chitosan edible films on cherry tomatoes. Compared with control samples (tomatoes without a coating and those coated with quinoa protein/chitosan), tomatoes with this coating and inoculated with *B. cinerea* showed a significant decrease in fungal growth after 7 days at 5 °C (Robledo et al., 2018).

The aim of the present work was to improve the performance of quinoa protein/chitosan edible films on the extension of postharvest life of blueberries and tomato cherries. For this purpose, chitosan thymol NPs were obtained by ionic gelation, and their effectiveness was evaluated against *Botrytis cinerea*. These NPs were included in the composite film, and its performance on reducing water vapour permeability was evaluated. Finally, this nanocomposite film was applied as an internal coating to a PET (polyethylene terephthalate) clamshell container to store blueberries and cherry tomatoes, and the weight loss was evaluated.

2. Materials and methods

2.1. Materials

Quinoa flour (*Chenopodium quinoa* Willd.) was supplied by "Cooperativa Las Nieves" (VI Region of Chile). The flour was stored at 4 °C until use. The flour was stored at 4 °C until use. The following is approximate composition of quinoa flour expressed in grams per 100 g: moisture 10.7 ± 0.2, protein 14.4 ± 0.2, fat 8.4 ± 0.1, ash 2.5 ± 0.1, and carbohydrates 64.0 (AOAC, 1995).

2.1.1. Chitosan

Chitosan films: Medium molecular weight chitosan (MMWC), with a deacetylation degree (DD) of 88.5% measured by proton nuclear magnetic resonance (NMR-H^1) and number average molecular weight (Mw_n) of 854 kDa measured by gel permeation chromatography (GPC) from crab shells, was obtained from Sigma Aldrich, USA (448877-250G).

Chitosan nanoparticles: Low molecular weight chitosan (LMWC) was purchased from Sigma Aldrich, Inc. (St. Louis, MO, USA, C448869), the following properties were measured: viscosity reduction (η_{sp}/c) = 203 (mL/g), viscosity average molar mass (Mv) = 269 kDa and deacetylation degree (DD) = 78.3%, as measured by NMR-H^1 (Lavertu et al., 2003). The intrinsic viscosity was determined in 0.1 M acetic acid (HOAc) + 0.2 M NaCl at 25 °C. The viscosity average molecular weight was determined using the Mark Howink constants in this solvent: K = 1.81E-03 mL/g and a = 0.93 (Rinaudo et al., 1993; Tapia et al., 2008).

2.1.2. Microbial strains

S. aureus ATCC 25923; *S. enterica serovar typhimurium* ATCC 14028; and *Listeria innocua* ATCC 33090 were obtained from the Instituto de Salud Pública, Santiago, Chile, and used for antimicrobial activity testing. Wild-type *B. cinerea* was isolated from Red Globe vines.

2.1.3. Blueberries and cherry tomatoes

Blueberries and cherry tomatoes were obtained from Hortifrut S.A, Chile and were taken to the laboratory keeping cold chain; experiments were carried out on the same day.

2.1.4. Other materials

Thymol (> 99.5%, product #T0501), tripolyphosphate pentasodium, (85%, product #238503), Pluronic F-127 (product #P2443) and dialysis tubing cellulose membrane (molecular weight cut-off = 14,000, product #D9402) were purchased from Sigma–Aldrich Co (USA).

2.2. Preparation of nanoparticles

Chitosan-thymol nanoparticles (CTNPs) were prepared by diluting 1.9 g of citric acid in 100 mL of 1 mg/mL of thymol in water. Then, 300 mg of LMWC was added to the mixture and left overnight with stirring. Chitosan nanoparticles (CNPs) were prepared by diluting 300 mg of LMWC in citric acid solution (1.9 g/100 mL). The chitosan-thymol or chitosan solution was filtered through a 0.45-μm membrane and loaded into two 50-mL syringes mounted on an infusion pump (Model KDS200; KD Scientific®, Holliston, MA). The solution was pumped at a rate of 1.8 mL/min over 50 mL of an aqueous solution of sodium TPP at 0.1% (w/v). The resulting suspension was centrifuged at 24,000 × *g* for 30 min. The supernatant of NPs was stored at 4 °C until use.

2.3. Characterization of NPs

Zeta potential, polydispersity index and particle hydrodynamic diameter: Samples of fresh supernatant of NPs with thymol (CTNP) and without thymol (CNP) were used to determine the zeta potential, PDI, and particle hydrodynamic diameter at 25 °C using a Zetasizer Nano ZS-20 (Malvern instruments) operating at 4.0 mW and 633 nm, with a fixed scattering angle of 173°.

Transmission electron microscopy (TEM) analysis: A Philips Tecnai 12 Bio Twin transmission electron microscope was used to observe the morphology of the NP. One drop of fresh supernatant of NP was spread onto a coated copper grid, which was then dried at room temperature prior to TEM analysis.

Powder X-ray Diffraction: X-ray diffraction was performed using a Siemens D-5000 powder X-ray diffractometer with CuKα radiation (λ 1.54 Å; 0.02). A theta range of 1.7–80 was selected to analyse the crystal structure. X-ray analyses were performed on lyophilized samples of NPs.

2.4. Parameters of encapsulation

A sample of a supernatant of CTNP was dialysed against water for 150 min (with a dialysis tubing cellulose membrane with a molecular weight cut-off of 14,000). The obtained dialysate was analysed by UV spectrophotometry at 273 nm [according to the thymol determination method described by Garsuch and Breitkreutz (2010) and Pan et al. (2014)]; the dialysate obtained from the CNP supernatant served as a blank. A dialysated sample was lyophilized in a plastic Petri dish with 13.5-cm diameter, covered with a layer of aluminium foil perforated at −55 °C and 6.7 Pa, for a period of 2 days. Subsequently, the sample was ground in a porcelain mortar and then stored at 4 °C.

The parameters of encapsulation were calculated as follows:

$$\%EE = \frac{mass\ of\ Thy\ in\ the\ supernant\ dialysated}{Initial\ Thy\ mass\ added} x100 \quad (1)$$

Where:

% EE: Efficiency of encapsulation
Thy: thymol

$$\%LC = \frac{mass\ of\ Thy\ in\ the\ supernant\ dialysated}{mass\ of\ the\ lyophilized\ sample\ of\ the\ supernant\ dialysated} x100 \quad (2)$$

Where:

% LC: Loading capacity
Thy: thymol

$$\%YP = \frac{mass\ of\ the\ lyophilized\ sample\ of\ the\ supernant\ dialysated}{mass\ of\ initial\ ingredients\ added} x100 \quad (3)$$

Where:

% YP: Yield particles

2.5. Antimicrobial activity of NP against bacterial strains

Preparation of inoculum: *S. aureus, S. typhimurium and L. innocua* were each cultured in 10 mL of tryptone soy broth (TSB) and incubated in a shaker incubator at 37 °C for 24 h. The optical density of the bacteria was adjusted to 0.5 on the standard of McFarland scale. The final concentration of the cells obtained was approximately 10^5–10^6 CFU/mL.

Antimicrobial activity by disc diffusion method: The agar diffusion method was used to determine the antibacterial performance of the CTNP for the three bacterial strains used in this study according to the standard methodology (Bauer et al., 1966; Sambrook et al., 1989). Filter paper discs with a 6.0 mm diameter and a thickness of 0.65 mm were coated with 10 µl of fresh supernatant of NPs with and without the addition of thymol. Three solutions were used as controls: a LMW chitosan solution, a thymol solution, and a blend solution of LMWC and thymol with equivalent amounts of T than the present in the NPs (with a concentration of LMWC and T of 0.7 mg/mL and 2 mg/mL, respectively). The discs were tested for their inhibition against *L. innocua* (Gram-positive), *S. aureus* (Gram-positive) and *S. typhimurium* (Gram-negative). Müller-Hinton agar plates were inoculated at levels of 10^6 CFU/mL of bacteria mentioned above, and discs containing the NPs were placed on the surface of the plate. After incubation at 37 °C for 24 h, the clear zone that formed in the medium around the disc was measured and recorded as the zone of inhibition of the microbial species.

2.6. Antimicrobial activity of NP against mycelia growth of Botrytis cinerea

The inhibition of radial mycelia growth by the CTNP was evaluated according to Yildirim and Yapici (2007). Different dilutions of NPs were dissolved in previously autoclaved potato dextrose agar to final concentrations of 0 (viability control), 10, 25, and 50% v/v (see Table 1) and were immediately poured into 9-cm-diameter Petri plates. A blended solution of LMWC and thymol with equivalent amounts of T and NPs was used as the control. Agar plugs (5 mm in diameter) were taken from the periphery of an 8-day-old culture of *Botrytis cinerea* that had been previously cultivated and transferred to the centre of the plates. Dishes were incubated for 8 days at 25 °C. *In vitro* activity of NPs was determined by comparing the mm of mycelia growth between the viability control plate (100% of growth) and the mm of mycelia growth in those with NPs.

Table 1
Chitosan and chitosan thymol nanoparticles (CNPs and CTNPs), and chitosan thymol physical blend (CT) solutions at different concentrations.

Antifungal compounds	Thymol (T) (mg mL^{-1})	Chitosan (C) (mg mL^{-1})
CNPs 10%	0.0	0.2
CNPs 25%	0.0	0.4
CNPs 50%	0.0	0.9
CTNPs 10%	0.1	0.2
CTNPs 25%	0.2	0.4
CTNPs 50%	0.3	0.9
Blend CT 10%	0.1	0.2
Blend CT 25%	0.2	0.5
Blend CT 50%	0.3	1.0

2.7. Preparation of films

The film solutions were prepared according to Valenzuela et al. (2013a, b). Control films (CQF) were prepared as follows: a solution of medium molecular weight chitosan (MMWC) at 2% w/v in citric acid 0.1 M was mixed with a quinoa solution (0.72 g of protein per 100 mL) at pH 11 at an equal mass ratio using a blade homogenizer (Bosch MSM6A3R 750w, China). For films with sunflower oil (CQOF), the MMWC-quinoa solution described above was blended with 2.9% w/v of sunflower oil and Tween 80 at 0.6% w/v with a high-speed Ultraturrax (Silverson L4R Machines, UK) for 10 min at 10,000 rpm. For films with CTNP (CQTF), the solvent used to prepare the chitosan solution at 2% w/v was the supernatant of CTNP described in section 2.2. CQTF was prepared at two proportions, 1% and 5%, based on the mass ratio between CTNP and chitosan presents in the film. The pH of the mixtures was adjusted to 3.0 with 1 M citric acid, and stirring was continued for 30 min. Then, the mixture was cast in low-density polyethylene Petri dishes boxes and dried to a constant weight at 50 °C. The final moisture content of the films was 8.46% ± 0.6% **(dry basis),** without significant differences among the film samples. The dried films were removed and conditioned in an environmental chamber (Model LTH-0150E, Labtech, Co., Korea) at 23 °C and 60% relative humidity for 48 h.

2.7.1. Film characterization

The microstructure of the films was observed by scanning electron microscopy (SEM) on a Hitachi TM table-top microscope (Software TM3000). The films were mounted in a 10-mm-diameter cylindrical die using double-sided adhesive tape and were then gold-sputter-coated for 3 min at 20 kV in an argon atmosphere (PELCO 91000) to render them electrically conductive.

The mechanical properties of the films were measured in a universal tensile testing machine (LLOYD model LR5K, England) provided with a 500 N load cell. The tensile strength (TS) and percent elongation at break (%E) were determined using the Official Chilean Standard method (NCh1151, 1999), which is equivalent to the ISO R1184-1970 standard method. Film samples were cut into 10 mm × 50 mm strips and tested using a double clamp with a separation of 30 mm at a test speed of 20 mm/min. The TS and %E values reported are the average of at least four measurements performed for each type of film.

The water vapour permeability (WVP) tests were carried out according to the Official Chilean Standard method (NCh 2098, 2000), which is equivalent to the ASTM D1653-93 and DIN 52615 standard methods, using the wet cup method and testing six films of each sample. The cup was filled with distilled water to a height of 6 mm from the top edge. The film was sealed to the cup with silica gel. The cup was placed in refrigerated chamber modular with evaporators at 0 ± 0.6 °C and 85 ± 2% relative humidity. The weight of the cup was measured daily for 21 days. The WVP was estimated according to McHugh et al. (1993).

2.8. Treatment application on clamshell to store the fruits

The fruits were randomly categorized into two groups, with 30 blueberries (± 87 g) or 15 cherry tomatoes (± 150 g) per treatment, and each treatment was conducted with three replicates. One of these groups was assigned to internal coating of the commercial PET perforated retail clamshell (Airpack 230 g capacity) with CQT films solution (named as CC), and the other group was assigned to the control clamshell without internal coating (named control). The PET clamshell boxes with internal coating were previously prepared by a double homogenous layer application of the film solution (CQT) over the inner faces of the clamshell. A manual air brush was employed for coating the internal area of the clamshell. A double internal coating with airbrush was carried out. The application method consisted of aspersion of the film solution on the internal surface (6 faces), and to dry at room temperature for 1 h, then the aforementioned application was repeated. Finally, fruit samples were stored at 7 ± 1 °C and 85% RH for 10 days.

2.8.1. Weight loss percentage

Each clamshell unit of each group (CC and control) was weighed at the beginning of the experiment (day 0) and during the storage period (day 6 and day 9). Weight was recorded using a scale with an accuracy of 0.01 g and was expressed as accumulated weight loss percentage per unit time.

2.9. Statistical analysis

Each experiment was conducted a minimum of three times, and each analysis was carried out in triplicate. The experimental data were subjected to analysis of variance, and significant differences between means were evaluated by Tukey's multiple-range test (Statgraphics, version 5.0; Statpoint Technologies, Inc. Warrenton, Virginia). A p value < 0.05 was considered statistically significant.

3. Results and discussion

3.1. Characterization of nanoparticles

NPs without thymol were prepared using a chitosan solution at 3.0 mg/mL, with a molecular weight of 269 kDa, DD of 78%. Chitosan/tripolyphosphate (C/TPP) mass ratio was 6/1, and the pH of the reaction was 4.1. Under these conditions, NPs with a hydrodynamic diameter (Z average = 175 ± 21) similar to the diameter measured by TEM (153 ± 42) were obtained. The Polydispersity index (PDI) value was 0.4 ± 0.1, and the Z potential was 37 ± 2.7 mV, see Table 2.

Antoniou et al. (2015) found that the size, PDI and Z potential of CNP are highly dependent on the concentration and molecular weight of chitosan, C/TPP mass ratio, and pH of the reaction. Rampino et al. (2013) used a C/TPP mass ratio of 6, chitosan solution at 2.5 mg/mL and a chitosan Mw of 150 kDa and obtained CNP with a Z average of approximately 200 nm. Koukaras et al. (2012) prepared NPs using chitosan solution at 2.0 mg/mL and a chitosan Mw of 350 kDa obtaining a Z average of approximately 500 nm at the same C/TPP mass ratio. The previously published results indicate that when a higher concentration of chitosan, close to its critical concentration of coil overlap (2.5 mg/mL; Rampino et al., 2013), and high-molecular-weight chitosan are used, the size, PDI, and Z potential all increase.

Keawchaoon and Yoksan (2011) reported CNP loaded with carvacrol, which is an isomer of thymol. These CNP were obtained using a chitosan solution at 12 mg/mL and chitosan MW of 760 kDa. The C/TPP mass ratio used was 2.4/1, and they used Tween 60 before gelification with TPP. Compared with our work, they reported a higher Z average (520 nm) and Z potential (42 mV). This difference is explained by the higher concentration and molecular weight of chitosan used. Their work examined a series of different weight ratios of chitosan to carvacrol from 1/0.25 to 1/1.25. The EE and LC of carvacrol ranged from approximately 13.6–27.8% and 2.7–21.2%, respectively, for C/carvacrol, and the mass ratio ranged from 1/0.25 to 1/1.125. The Z average of NPs ranged from approximately 518-716 nm, and the average diameter obtained by TEM was 40–80 nm. The Z potential of NP without carvacrol was approximately 42 mV, but this value diminished drastically to approximately 25–29 mV when carvacrol was added. This diminished was not proportionality related with the mass ratio C/carvacrol.

This study used a C/T mass ratio of 1/0.33, see Table 2. NPs with thymol showed a significantly lower size, as measured by DLS (Z average = 293 ± 37 nm), compared with the values obtained by Keawchaoon and Yoksan (2011). The size measured by TEM was similar (diameter average = 204 ± 43 nm). This difference is probably due to the lower MW, 269 kDa, and concentration, 3.0 mg/mL, of chitosan, and higher C/TPP, 6/1, used in the procedure. Consequently, with a lower Z average of 293 nm, the Z potential was significantly higher, at 47 mV. The effect of thymol on Z potential was opposite to the effect observed for carvacrol. The values of encapsulation of thymol were EE = 66.6% and LC = 2.5%. The values for carvacrol in a similar system for C/carvacrol at a mass ratio of 1/0.25 were EE = 13.6% and LC = 2.7%. Thus, the EE for thymol was higher than that for carvacrol, and the LC was lower. This difference could be explained by the higher C/TPP mass ratio (6/1) used for the encapsulation of thymol compared with the C/TPP mass ratio (2.4/1) used for carvacrol. The morphology of CTNP analysed by TEM, as shown in Fig. 1, was rounded and less aggregated compared with the previously described NPs, which were obtained using a high chitosan concentration solution (12 mg/mL) and high molecular weight (760 kDa) (Keawchaoon and Yoksan, 2011), but was similar to those described by Antoniou et al. (2015), who produced NPs with a low chitosan concentration solution (1.5 mg/mL) and low molecular weight (100 kDa).

Fig. 2 shows the X-ray powder diffraction (XRPD) patterns for chitosan, physical mixture of the components in the same proportion used in the CTNP. Additionally, the percentage of crystallinity of each system was estimated. The physical mixture had 16.2% of crystallinity, chitosan had 21.2%, and CTNP had the highest crystallinity of 51.1%. Two signals at 4.28 2θ and 6.5 2θ appeared in CTNP that could be associated with a modification of nanometric order in the internal structure when thymol is loaded in CNP. These signals are characteristics of the laminar structures observed in clays; the distances in these lamina were 2.06 nm and 1.6 nm, respectively (Shahbazi et al., 2017).

Table 2
Particle size (Z average, D*), polydispersity index (PDI), Z potential, yield particle (YP), encapsulation efficiency (EE) and loading capacity (LC) of chitosan and chitosan thymol nanoparticles (CNPs and CTNPs). Different letters indicate significant differences ($p < 0.05$).

Nanoparticles	Z average nm	D* nm	PDI	Z potential mV	YP %	EE %	CC %
CNPs	174.8 ± 21.4[a]	152.5 ± 42.0[a]	0.4 ± 0.1[a]	37.0 ± 2.7[a]	60.6 ± 1.3[a]	–	–
CTNPs (1/0.33 m/m)	293.1 ± 36.9[b]	204.4 ± 43.1[b]	0.5 ± 0.0[b]	47.8 ± 2.8[b]	89.8 ± 1.0[a]	66.6 ± 1.2	2.5 ± 0.0

*Obtained from TEM.

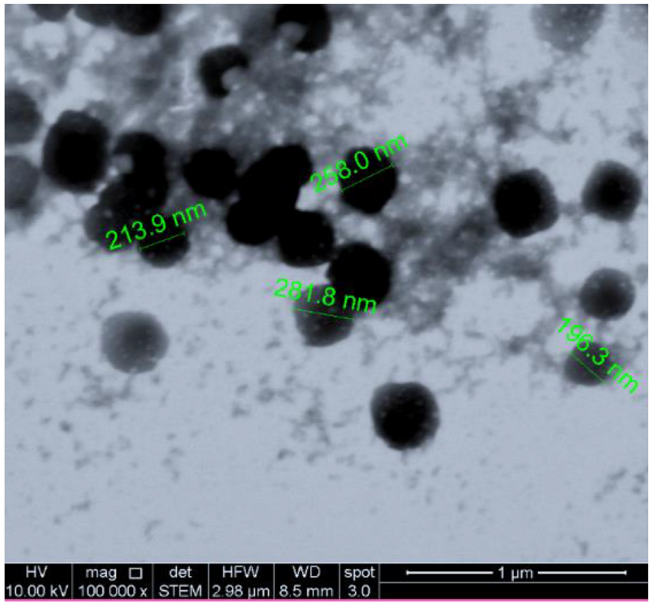

Fig. 1. Transmission electron microscopy image of chitosan-thymol nanoparticles (CTNPs).

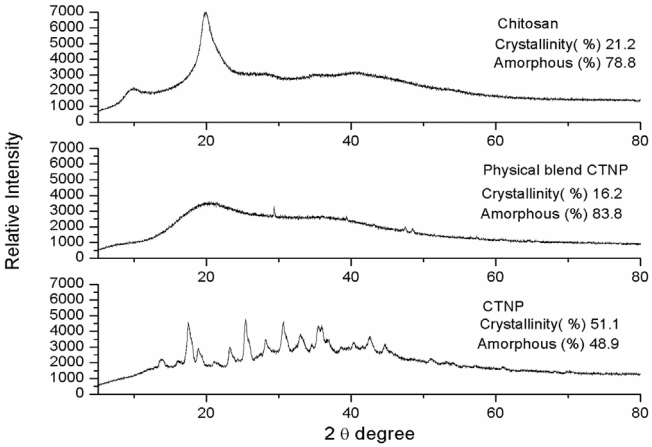

Fig. 2. X-ray diffraction profiles and crystallinity degree of chitosan, physical blend and nanoparticles CTNPs.

3.2. Antimicrobial activity of nanoparticles

The agar diffusion method was used to determine the antibacterial performance of the CTNP for a Gram-negative bacterium, *Salmonella typhimurium*, and two Gram-positive bacteria, *Staphylococcus aureus* and *Listeria innocua*; the results are shown in Table 3. Chitosan-Thymol NPs had a significantly greater inhibitory effect than did CNP and the control solutions on the three strains tested. For *S. aureus*, the zone of growth inhibition with CTNP treatment was 13.0 ± 1.9 mm^2, which was 31% above that of the blend CT control solution (9.93 ± 0.6 mm^2). The CTNP treatment on *L. innocua* showed a growth inhibition of 12.6 ± 3.0 mm^2, 64% above that of the blend CT solution (7.7 ± 1.0 mm^2), and for *S. typhimurium*, the same effect was observed, with a zone of growth inhibition value of 12.4 ± 1.8 mm^2, 26% above that of CT solution (9.9 ± 0.7 mm^2). These results are in accordance with those reported by Caro et al. (2016), who demonstrated a synergistic effect between C and T in NPs (obtained under same conditions of this report) and found that the minimum inhibitory concentration (MIC) for CTNP was approximately 1.5- to 4.5-fold lower than the theoretical MIC (which was calculated on the basis of an additive effect of MIC of C and T separately). This synergistic effect is attributed to the fact that C and T have different mechanisms of antimicrobial inhibition. Hosseinnejad and Jafari (2016) summarized several mechanisms for the antimicrobial activity by chitosan: 1) Positively charged chitosan molecules interfere with the negatively charged residues on the bacterial surface, leading to alterations in cell permeability; 2) The interaction of diffused hydrolysis products with microbial DNA, which leads to the inhibition of the mRNA and protein synthesis; 3) Inhibition of microbial growth by the chelation of nutrients and essential metals; 4) On the cell surface, chitosan can form a polymer membrane that prevents nutrients from entering the cell or can act as an oxygen barrier that inhibits the growth of aerobic bacteria. In contrast, the antimicrobial effect of T is due to its lipophilic nature; its activity occurs at the lipid level, and the enzymatic complexes of the membrane can alter the permeability and/or inhibit the cellular respiratory chain (Marei et al., 2012).

The inhibition of radial mycelia growth of Botrytis cinerea by the CTNPs, CNPs and chitosan/thymol (CT) blend solution was evaluated according to Yildirim and Yapici (2007) method. Each of the formulations were tested in different dilutions added to the potato dextrose agar (10, 25 and 50% v/v), which contained the same concentration of active compound (Chitosan and Thymol) in the final dilution (mg/mL) agar. The results of the inhibition of radial mycelial growth of *Botrytis cinerea* are shown in Table 4. CTNPs formulation showed 100% inhibition for all dilutions (10, 25 and 50%) in agar tested, whereas the CT blend solution showed total inhibition only at a higher concentration (50% v/v). CNP showed the lowest inhibition of mycelia growth at lowest dilutions, 10 and 25% (v/v), achieving an inhibition of 26 ± 1 and 50 ± 0%, respectively, while that at higher concentration 50% (v/

Table 3
Zone of growth inhibition by radial diffusion method of chitosan and chitosan thymol nanoparticles (CNPs and CTNPs), thymol (T) and chitosan (C) solutions at different concentrations. Different letters indicate significant differences ($p < 0.05$).

Treatment	T (mg mL^{-1})	C (mg mL^{-1})	Zone of growth inhibition (mm^2)		
			S. aureus	*L. innocua*	*S. typhimurium*
CTNPs	0.6	1.8	13.01 ± 1.9^{c}	12.63 ± 3^{b}	12.44 ± 1.8^{c}
CNPs	0.0	1.8	10.62 ± 0.5^{b}	8.17 ± 1^{a}	9.55 ± 1^{b}
T solution	0.7	0.0	7.54 ± 1.1^{a}	6.35 ± 1^{a}	5.91 ± 0.8^{a}
C solution	0.0	2.0	6.79 ± 0.1^{a}	6.60 ± 0.9^{a}	6.28 ± 0.5^{a}
Blend CT solution	0.7	2.0	9.93 ± 0.6^{b}	7.71 ± 1^{a}	9.86 ± 0.7^{b}

Table 4
Inhibition of radial mycelia growth of *Botrytis cinerea* by the chitosan and chitosan thymol nanoparticles (CNPs and CTNPs), and chitosan thymol blend (CT) solutions at different concentrations. Different letters indicate significant differences ($p < 0.05$).

Formulation	Concentration of formulation added to agar (%v/v)	Active compounds in formulation added to agar in final dilution (mg/mL)		Inhibition of radial mycelia growth in agar plates (%)
		Thymol (T)	Chitosan (C)	
CNPs	10	0.0	0.2	26 ± 1^{e}
	25	0.0	0.4	50 ± 0^{d}
	50	0.0	0.9	74 ± 5^{b}
CTNPs	10	0.1	0.2	100 ± 0^{a}
	25	0.2	0.4	100 ± 0^{a}
	50	0.3	0.9	100 ± 0^{a}
CT Blend solution	10	0.1	0.2	65 ± 4^{c}
	25	0.2	0.5	69 ± 6^{bc}
	50	0.3	1.0	100 ± 0^{a}

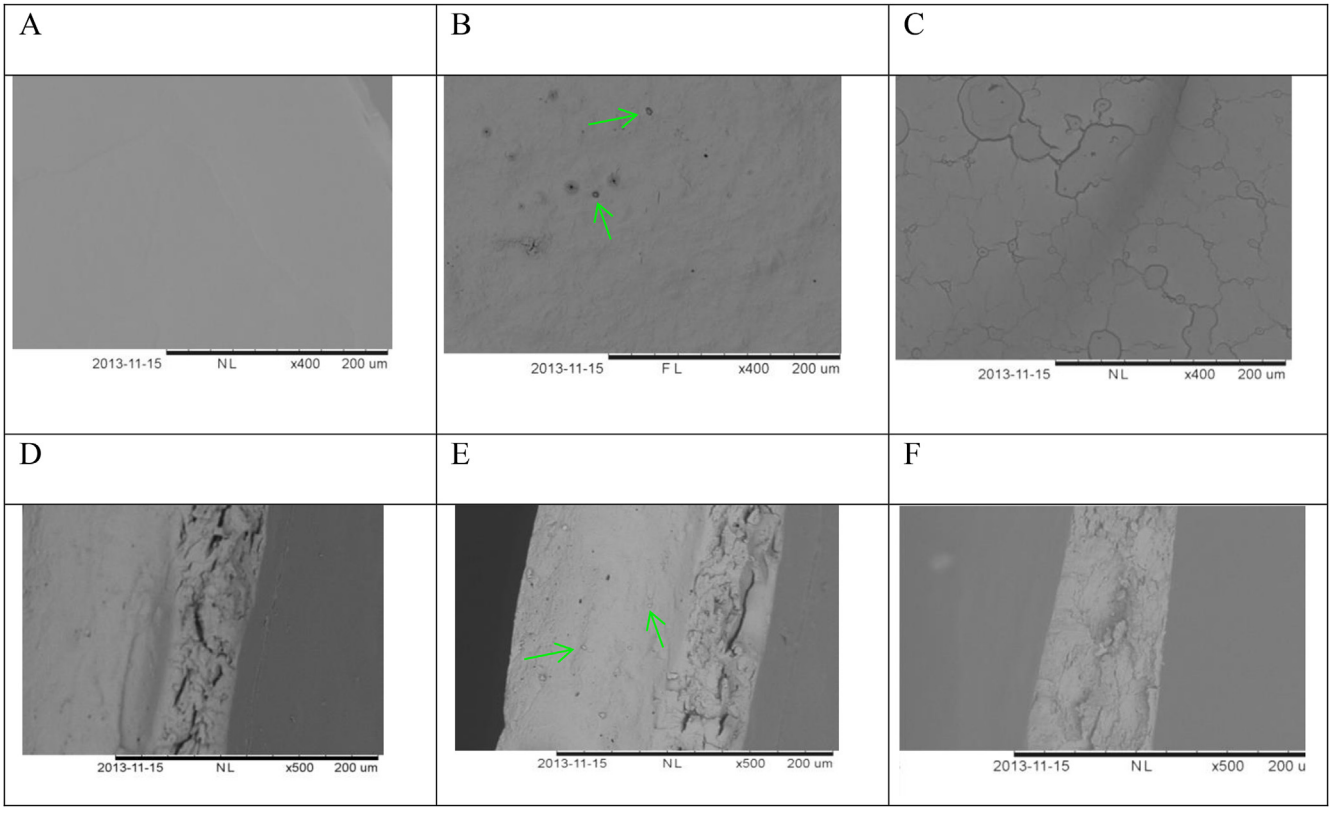

Fig. 3. Scanning electron micrographs of surfaces chitosan quinoa protein films: (a) film without NPs, (b) film with 5% NPs, (c) film with 2.9% sunflower seed oil. Scanning electron micrographs of cross section of quinoa chitosan blend films: (d) film without NPs, (e) film with 5% NPs, (f) film with 2.9% sunflower seed oil.

v) inhibits the 75 ± 5% of radial mycelia growth. This results pointed out a synergistic effect of nanoparticulated system (CTNP) compared with blend CT solution and the vehicle (CNP). Therefore, the CTNPs was the only treatment that showed an inhibitory effect at the lowest doses (10% dilution).

3.3. Film characterization

Surface and cross section SEM images of CQTF films with 5% CTNP (CQTF5), control CQ films (CQF), and CQ films with 2.9% oil (CQOF) are shown in Fig. 3. The CQTF films show irregularities, as shown by the arrows in Fig. 3b and e, compared with the smoothed surface of CQ films; see Fig. 3a. These irregularities can be attributed to the presence of NPs because these problems have been reported by Sun et al. (2014).) regarding starch films reinforced with $CaCO_3$ NPs. For CQ films with oil, a heterogeneous surface is observed (Fig. 3c and f). The cross section of the films shows a homogeneous distribution of CTNPs for CQTF5. The mechanical properties and WVP of CQTF films with 1% and 5% CTNPs (CQTF1, CQTF5), CQF, and CQOF are shown in Table 5. As observed in Table 5, the tensile strength of CQTF1 was the highest, and that of CQOF was the lowest, so the incorporation of 1% of CTNPs enhanced the CQ film matrix without impacting its % elongation at break. CQTF5 showed similar mechanical properties to CQF. Chang et al. (2010) explained this behaviour as an interfacial interaction between CNPs with its similar biopolymeric matrix, so CTNPs could act as a filler. The incorporation of CTNPs into CQ films significantly decreased ($p < 0.05$) the WVP of the films, but we did not observe a significant difference in the concentration of NPs (CQTF1 and CQTF5). The percentage reduction of WVP in group CQTF1 relative to the control CQF was approximately 17%, see Table 5; this decrease was higher than that observed for CQOF, which had only an 8% WVP reduction. The decrease in WVP by the incorporation of NPs into the films can be attributed to the homogeneous distribution of NPs in the polymer CQ matrix, which produces a tortuous path to the diffusion of water vapour across the films (Abdollahi et al., 2013; de Moura et al., 2009; Duncan, 2011).

Table 5
Mechanical and water vapour permeability properties of films of chitosan/quinoa protein (CQF), chitosan/quinoa protein with nanoparticles (CQTF), and chitosan/quinoa proteins with sunflower oil (CQOF). Different letters indicate significant differences ($p < 0.05$).

Films*	Elongation at break (%)	Tensile strength (N/mm^2)	Water vapour permeability (WVP) (g.mm.Pa^{-1} day^{-1} m^2)	% of diminished of WVP**
CQF	36.9 ± 12.28^{bc}	6.9 ± 1.46^{b}	0.41 ± 0.014^{c}	0^{c}
CQTF1	40.2 ± 9.18^{c}	7.8 ± 1.36^{c}	0.34 ± 0.025^{a}	−17^{a}
CQTF5	33.2 ± 11.29^{b}	6.3 ± 2.21^{b}	0.33 ± 0.027^{a}	−20^{a}
CQOF	26 ± 9.48^{a}	3.6 ± 0.97^{a}	0.38 ± 0.016^{b}	-7^{b}

*Film composition (g/100 mL): CQF (MMWC: 1.0; Quinoa protein: 0.36); CQTF1 (MMWC: 1.0; Quinoa protein: 0.36; CTNPs: 0.010); CQTF5 (MMWC: 1.0; Quinoa protein: 0.36; CTNPs: 0.025); CQOF (MMWC: 1.0; Quinoa protein: 0.36; sunflower oil: 1.45; TWEEN 80: 0.29).
** % of diminished of WVP was calculated in relation with the film control CQF.

3.4. Treatment application on fruits

The fruits' weight loss during storage is caused by the water loss due to fruit transpiration, which can be modified by changing the storage environment. As shown in Fig. 4, all samples experienced weight loss during the days of storage and showed significant differences between storage times ($p < 0.05$). Fruits stored in clamshells with internal coating with CTNP (CC) had a lower weight loss at days 5 and 9 of the study (Fig. 4). The weight loss for blueberries stored in CC was

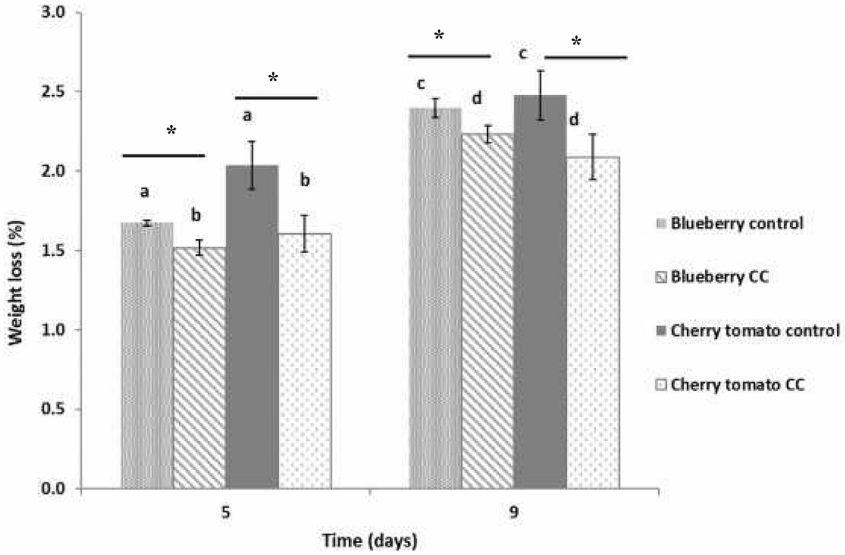

Fig. 4. Weight loss (in percentage) of blueberry and cherry tomato stored in clamshells with (CC) and without inner covering (control), stored at 7 °C. Values with different letters are significantly different ($p < 0.05$), comparison was made within same storage time.

approximately 12% and 8% lower than that in the control on days 5 and 9, respectively. The weight loss for tomato cherry stored in CC was 1.6% and 2.1% (day 5 and 9, respectively), whereas the control was 20% higher in both cases. The use of CC to store fruits allowed a lower weight loss and showed significant differences ($p < 0.05$) compared with the fruit stored in control clamshell. It has been reported that grapes coated with CNP obtained by ionic gelation show lower weight loss when stored at 0 °C for 60 days (Melo et al., 2018). It is likely that the water evaporated from the fruit is absorbed by chitosan due its hygroscopicity. Thus, chitosan formed a water barrier between the fruit and external environment, reducing the external transfer of water (Morillon et al., 2002; Olivas and Barbosa-Canovas, 2005; Xu et al., 2007).

4. Conclusion

NPs with thymol had a significantly greater inhibitory effect than did NPs without thymol or the control solutions over *Salmonella typhimurium*, *Staphylococcus aureus* and *Listeria innocua*. They were also effective in inhibiting the radial mycelia growth of *Botrytis cinerea*. The addition of 1% of NPs with thymol to chitosan-quinoa films improved the water barrier properties of the chitosan-quinoa protein film matrix without affecting its % elongation at break. The use of this mixture as an internal coating for clamshells containing cherry tomato and blueberries significantly reduced the weight loss.

Acknowledgement

This work was supported by INNOVA CORFO Project 12IDL-13621.

References

Abdollahi, M., Alboofetileh, M., Behrooz, R., Rezaei, M., Miraki, R., 2013. Reducing water sensitivity of alginate bio-nanocomposite film using cellulose nanoparticles. Int. J. Biol. Macromol. 54, 166–173. https://doi.org/10.1016/j.ijbiomac.2012.12.016.

Abugoch, L.E., Tapia, C., Villaman, M.C., Yazdani-Pedram, M., Diaz-Dosque, M., 2011. Characterization of quinoa protein-chitosan blend edible films. Food Hydrocolloids 25 (5), 879–886. https://doi.org/10.1016/j.foodhyd.2010.08.008.

Antoniou, J., Liu, F., Majeed, H., Qi, J., Yokoyama, W., Zhong, F., 2015. Physicochemical and morphological properties of size-controlled chitosan-tripolyphosphate nanoparticles. Colloid. Surface. Physicochem. Eng. Aspect. 465, 137–146. https://doi.org/10.1016/j.colsurfa.2014.10.040.

AOAC 942.15, 1995. Official Methods of Analysis of AOAC International, sixteenth ed. AOAC International, Gaithersburg, MD.

Bauer, A.W., Kirby, W.M., Sherris, J.C., Turck, M., 1966. Antibiotic susceptibility testing by a standardized single disk method. Am. J. Clin. Pathol. 45 (4), 493–496.

Bazile, D., Bertero, D., Nieto, C., 2014. State of the Art Report on Quinoa Around the World in 2013. Food and Agriculture Organization of the United Nations (FAO). Santiago. Centre de Coopération Internationale en Recherche Agronomique pour le Développement (CIRAD) Montpellier.

Caro, N., Medina, E., Diaz-Dosque, M., Lopez, L., Abugoch, L., Tapia, C., 2016. Novel active packaging based on films of chitosan and chitosan/quinoa protein printed with chitosan-tripolyphosphate-thymol nanoparticles via thermal ink-jet printing. Food Hydrocolloids 52, 520–532. https://doi.org/10.1016/j.foodhyd.2015.07.028.

Chang, P.R., Jian, R.J., Yu, J.G., Ma, X.F., 2010. Fabrication and characterisation of chitosan nanoparticles/plasticised-starch composites. Food Chem. 120 (3), 736–740. https://doi.org/10.1016/j.foodchem.2009.11.002.

de Moura, M.R., Aouada, F.A., Avena-Bustillos, R.J., McHugh, T.H., Krochta, J.M., Mattoso, L.H.C., 2009. Improved barrier and mechanical properties of novel hydroxypropyl methylcellulose edible films with chitosan/tripolyphosphate nanoparticles. J. Food Eng. 92 (4), 448–453. https://doi.org/10.1016/j.jfoodeng.2008.12.015.

Dehnad, D., Emarn-Djomeh, Z., Mirzaei, H., Jafari, S.M., Dadashi, S., 2014. Optimization of physical and mechanical properties for chitosan-nanocellulose biocomposites. Carbohydr. Polym. 105, 222–228. https://doi.org/10.1016/j.carbpol. 2014.01.094.

Duncan, T.V., 2011. Applications of nanotechnology in food packaging and food safety: barrier materials, antimicrobials and sensors. J. Colloid Interface Sci. 363 (1), 1–24. https://doi.org/10.1016/j.jcis.2011.07.017.

Fuentes, F., Olguin, P., Duarte, A., Ojeda, M., Martínez, E., Paredes, X., Figueroa, C., Pérez, C., 2017. Fundación para la Innovación Agraria (FIA) Potential competitivo de la quinua chilena.

Garsuch, V., Breitkreutz, J., 2010. Comparative investigations on different polymers for the preparation of fast-dissolving oral films. J. Pharm. Pharmacol. 62 (4), 539–545. https://doi.org/10.1211/jpp.62.04.0018.

Hosseinnejad, M., Jafari, S.M., 2016. Evaluation of different factors affecting antimicrobial properties of chitosan. Int. J. Biol. Macromol. 85, 467–475. https://doi.org/10.1016/j.ijbiomac.2016.01.022.

Keawchaoon, L., Yoksan, R., 2011. Preparation, characterization and in vitro release study of carvacrol-loaded chitosan nanoparticles. Colloids Surfaces B Biointerfaces 84 (1), 163–171. https://doi.org/10.1016/j.colsurfb.2010.12.031.

Kerch, G., 2015. Chitosan films and coatings prevent losses of fresh fruit nutritional quality: a review. Trends Food Sci. Technol. 46 (2), 159–166. https://doi.org/10.1016/j.tifs.2015.10.010.

Koukaras, E.N., Papadimitriou, S.A., Bikiaris, D.N., Froudakis, G.E., 2012. Insight on the formation of chitosan nanoparticles through ionotropic gelation with tripolyphosphate. Mol. Pharm. 9 (10), 2856–2862. https://doi.org/10.1021/mp300162j.

Lavertu, M., Xia, Z., Serreqi, A.N., Berrada, M., Rodrigues, A., Wang, D., Gupta, A., 2003. A validated H-1 NMR method for the determination of the degree of deacetylation of chitosan. J. Pharmaceut. Biomed. Anal. 32 (6), 1149–1158. https://doi.org/10.1016/S0731-7085(03)00155-9.

Marei, G.I.K., Rasoul, M.A.A., Abdelgaleil, S.A.M., 2012. Comparative antifungal activities and biochemical effects of monoterpenes on plant pathogenic fungi. Pestic. Biochem. Physiol. 103 (1), 56–61. https://doi.org/10.1016/j.pestbp.2012.03.004.

Melo, N., MendonçaSoares, B., Diniz, K., Leal, C., Canto, D., Flores, M., da Costa Tavares-Filho, J., Galembeck, A., Montenegro, T., Montenegro Stamford-Arnaud, T., Montenegro Stamford, C., 2018. Effects of fungal chitosan nanoparticles as eco-friendly edible coatings on the quality of postharvest table grapes. Postharvest Biol. Technol. 139, 56–66. https://doi.org/10.1016/j.postharvbio.2018.01.014.

Mirdehghan, S., Valero, D., 2017. Bioactive compounds in tomato fruit and its antioxidant activity as affected by incorporation of Aloe, eugenol, and thymol in fruit package during storage. Int. J. Food Prop. 20, 1798–1806. https://doi.org/10.1080/

10942912.2016.1223128.
McHugh, T.H., Avena-bustillos, R., Krochta, J.M., 1993. Hydrophilic edible films - modified procedure for water-vapor permeability and explanation of thickness effects. J. Food Sci. 58 (4), 899–903. https://doi.org/10.1111/j.1365-2621.1993.tb09387.x.
Morillon, V., Debeaufort, F., Blond, G., Capelle, M., Voilley, A., 2002. Factors affecting the moisture permeability of lipid-based edible films: a review. Crit. Rev. Food Sci. Nutr. 42 (1), 67–89. https://dx.doi.org/10.1080/10408690290825466.
Muller, C.M.O., Laurindo, J.B., Yamashita, F., 2009. Effect of cellulose fibers addition on the mechanical properties and water vapour barrier of starch-based films. Food Hydrocolloids 23 (5), 1328–1333. https://doi.org/10.1016/j.foodhyd.2008.09.002.
Muxika, A., Etxabide, A., Uranga, J., Guerrero, P., De la Caba, K., 2017. Chitosan as a bioactive polymer: processing, properties and applications. Int. J. Biol. Macromol. 105, 1358–1368. https://doi.org/10.1016/j.ijbiomac. 2017. 07.087.
NCh1151.Of76, 1999. Norma Chilena Oficial: Láminas Y Películas Plásticas. Determinación de las propiedades de tracción 13 pp.
NCh2098.Of2000, 2000. Norma Chilena Oficial: Películas de recubrimiento orgánico. Determinación de la transmisión de vapor de agua 13 pp.
Olivas, G., Barbosa-Cánovas, G., 2005. Edible coatings for fresh-cut fruits. Crit. Rev. Food Sci. Nutr. 45, 657–670. https://doi.org/10.1080/10408690490911837.
Pan, K., Chen, H.Q., Davidson, P.M., Zhong, Q.X., 2014. Thymol nanoencapsulated by sodium caseinate: physical and antilisterial properties. J. Agric. Food Chem. 62 (7), 1649–1657. https://doi.org/10.1021/jf4055402.
Rampino, A., Borgogna, M., Blasi, P., Bellich, B., Cesaro, A., 2013. Chitosan nanoparticles: preparation, size evolution and stability. Int. J. Pharm. 455 (1–2), 219–228. https://doi.org/10.1016/j.ijpharm.2013.07.034.
Rinaudo, M., Milas, M., Ledung, P., 1993. Characterization of chitosan - influence of ionic-strength and degree of acetylation on chain expansion. Int. J. Biol. Macromol. 15 (5), 281–285. https://doi.org/10.1016/0141-8130 (93) 90027-J.
Robledo, N., Vera, P., López, L., Yazdani-Pedram, M., Tapia, C., Abugoch, L., 2018. Thymol nanoemulsions incorporated in quinoa protein/chitosan edible films; antifungal effect in cherry tomatoes. Food Chem. 246, 211–219. https://doi.org/10.1016/j.foodchem.2017.11.032.
Sambrook, J., Fritsch, E.F., Maniatis, T., 1989. Molecular Cloning - a Laboratory Manual, second ed. (New York).
Shahbazi, M., Rajabzadeh, G., Ahmadi, S.J., 2017. Characterization of nanocomposite film based on chitosan intercalated in clay platelets by electron beam irradiation. Carbohydr. Polym. 157, 226–235. https://doi.org/10.1016/j.carbpol.2016.09.018.
Sun, Q., Xi, T., Li, Y., Xiong, L., 2014. Characterization of corn starch films reinforced with $CaCO_3$ nanoparticles. PLoS One 9 (9), e106727. https://doi.org/10.1371/journal. pone.0106727.
Tapia, C., Montezuma, V., Yazdani-Pedram, M., 2008. Microencapsulation by spray coagulation of diltiazem HCl in calcium alginate-coated chitosan. AAPS PharmSciTech 9 (4), 1198–1206. https://doi.org/10.1208/s12249-008-9164-3.
Valenzuela, C., Abugoch, L., Tapia, C., Gamboa, A., 2013a. Effect of alkaline extraction on the structure of the protein of quinoa (*Chenopodium quinoa* Willd.) and its influence on film formation. Int. J. Food Sci. Technol. 48 (4), 843–849. https://doi.org/10.1111/ijfs.12035.
Valenzuela, C., Abugoch, L., Tapia, C., 2013b. Quinoa protein-chitosan-sunflower oil edible film: mechanical, barrier and structural properties. LWT-Food Science and Technology 50 (2), 531–537. https://doi.org/10.1016/j.lwt.2012.08.010.
Vargas, M., Albors, A., Chiralt, A., Gonzalez-Martinez, C., 2009. Characterization of chitosan-oleic acid composite films. Food Hydrocolloids 23 (2), 536–547. https://doi.org/10.1016/j.foodhyd.2008.02.009.
Xin, Y., Chen, F., Lai, S., Yang, H., 2017. Influence of chitosan-based coatings on the physicochemical properties and pectin nanostructure of Chinese cherry. Postharvest Biol. Technol. 133, 64–71. https://doi.org/10.1016/j.postharvbio.2017.06.010.
Xu, W., Huang, K., Guo, F., Qu, W., Yang, J., Liang, Z., Luo, Y., 2007. Postharvest grapefruit seed extract and chitosan treatments of table grapes to control *Botrytis cinerea*. Postharvest Biolology and Technology 46, 86–94. https://doi.org/10.1016/j.postharvbio.2007.03.019.
Yildirim, I., Yapici, B., 2007. Inhibition of conidia germination and mycelial growth of Botrytis cinerea by some alternative chemical. Pakistan J. Biol. Sci. 10 (8), 1294–1300. https://doi.org/10.3923/pjbs.2007.1294.1300.